Site Transformation of Polyisobutylene Chain Ends into Functional RAFT Agents for Block Copolymer Synthesis

Andrew J. D. Magenau, Nemesio Martinez-Castro, and Robson F. Storey*

School of Polymers and High Performance Materials, The University of Southern Mississippi, 118 College Dr. #10076, Hattiesburg, Mississippi 39406

Received January 13, 2009; Revised Manuscript Received February 13, 2009

ABSTRACT: Block copolymers consisting of polyisobutylene (PIB) and either poly(methyl methacrylate) (PMMA) or polystyrene (PS) block segments were synthesized by a site transformation approach combining living cationic and reversible addition−fragmentation transfer (RAFT) polymerizations. The initial PIB block was synthesized via quasi-living cationic polymerization using the TMPCl/$TiCl_4$ initiation system and subsequently converted into a hydroxyl-terminated PIB. Site transformation of the hydroxyl-terminated PIB into a macro-chain-transfer agent (PIB−CTA) was accomplished by *N,N′*-dicyclohexylcarbodiimide/dimethylaminopyridine-catalyzed esterification with 4-cyano-4-(dodecylsulfanylthiocarbonylsulfanyl)pentanoic acid. Structure of the PIB-CTA was confirmed by both ^{1}H and ^{13}C NMR spectroscopy. The PIB−CTA was then employed in a RAFT polymerization of either methyl methacrylate or styrene, resulting in PIB block copolymers with narrow polydispersity index and predetermined molecular weights confirmed by both ^{1}H NMR and GPC.

Introduction

Polyisobutylene (PIB) is a fully saturated hydrocarbon elastomer with outstanding oxidative and chemical resistance, superior gas-barrier and mechanical damping characteristics, and excellent biocompatibility. Because of these characteristics, block copolymers based on PIB elastomeric segments are currently of great interest as self-assembling materials with unique properties. For example, PIB-based triblock copolymers have become an attractive candidate as a biomaterial and have found a niche market in this field.[1] Poly(styrene-*b*-isobutylene-*b*-styrene) (SIBS) is currently being used as a drug-eluting coating for coronary stents because of its effectiveness as a drug delivery matrix, vascular biocompatibility, and advantageous mechanical properties.[2,3] Faust et al. have studied drug release characteristics of similar materials possessing outer blocks derived from methyl methacrylate (MMA), 2-hydroxyethyl methacrylate (HEMA), and hydroxyl and acetylated styrene (S) derivatives.[4,5] Recently, much progress has been made in the synthesis of self-assembling PIB-based polymersomes and micelles to create new delivery/encapsulation systems and interpolyelectrolyte complexes for biotechnology and medicine.[6,7] In other application areas, Binder and Machl have synthesized poly(ether ketone-*b*-PIB-*b*-ether ketone) triblock copolymers with potential uses as high-temperature thermoplastic elastomers (TPEs) with outer block T_g's above 150 °C.[8] ABA rod−coil−rod triblock copolymers containing a PIB center block and mesogen-jacketed liquid crystalline polymer outer blocks exhibit liquid crystalline properties and have been suggested to have potential electrochemical applications.[9]

The examples above demonstrate that a number of methods have been devised for the creation of novel block copolymers, in addition to traditional sequential monomer addition. Specifically, the technique of site transformation can be used to greatly expand the library of polymer segments that can be mated to PIB to form new and interesting block copolymers. In this method, PIB block segments derived through cationic polymerization are converted into functional macroinitiators for a chain polymerization process other than cationic. For PIB-based systems this has typically involved combinations of living cationic polymerization with atom transfer radical polymerization (ATRP),[10−13] condensation polymerization,[14] or anionic polymerization.[15,16]

The relatively new controlled/living radical polymerization technique, reversible addition−fragmentation chain transfer (RAFT) polymerization, has proven to be very versatile regarding monomers, solvents, and reaction conditions to yield macromolecules with predetermined molecular weights and narrow polydispersities.[17] In addition, chain transfer agents (CTAs) used in the RAFT process can be synthesized to carry many useful reactive end groups. These end groups can later be used for coupling reactions to various macromolecules allowing for subsequent block copolymer synthesis.[18] This type of approach has been demonstrated with poly(ethylene glycol) (PEO),[19] commercially available Kraton polymers,[20] and solid polymer supports derived from cotton,[21] and was successfully used to convert these macromolecules into functional macro-CTA's for block and graft copolymer synthesis. Because of the versatility of RAFT polymerizations and its capability to polymerize many monomers that are inherently troublesome for other polymerization techniques, RAFT is potentially an ideal polymerization technique to combine with cationic polymerization by site transformation. This unique combination would allow the synthesis of a variety of PIB-based block copolymers with potentially new or greatly improved properties compared to what is currently available. Herein, we report an initial example of combining living cationic polymerization of isobutylene with the subsequent RAFT polymerization of methyl methacrylate (MMA) and styrene (S) through site transformation of PIB chain ends into functional macro-CTAs (Scheme 1). With these model monomers as a template, further expansion of this technique can be used for the synthesis of PIB-based copolymers with monomers traditionally inaccessible to PIB and cationic polymerization.

Experimental Section

Materials. Hexane (anhydrous, 95%), $TiCl_4$ (99.9%, packaged under N_2 in sure-seal bottles), 2,6-lutidine (redistilled, 99.5%), chloroform-*d* (99.8 atom % D), *N,N′*-dicyclohexylcarbodiimide (99%) (DCC), 4-(dimethylamino)pyridine (99%) (DMAP), anhydrous dichloromethane (99.8%) (DCM), 1,2,2,6,6-pentamethylpiperidine (97%) (PMP), and 1,3,5-trioxane (≥99%) were purchased from Sigma-Aldrich and used as received. Methyl methacrylate (MMA) (99%), benzene (≥99.0%), and styrene (S) (99.5%) were

* Corresponding author: e-mail Robson.Storey@usm.edu; Tel 601-266-4879; Fax 601-266-5635.

10.1021/ma900070d CCC: $40.75
Published on Web 03/11/2009

Scheme 1. Site Transformation from Living Carbocationic Polymerization to RAFT Polymerization

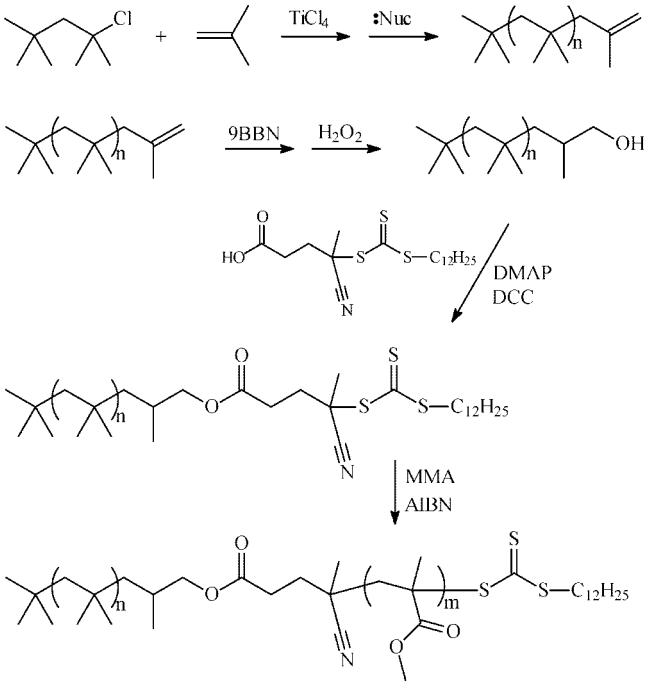

Table 1. Characterization of *exo*-Olefin PIB Precursors

sample	M_n[a] (g/mol)	PDI (M_n/M_w)	*exo*-olefin[b] (%)
PIB-1	1600	1.04	98
PIB-2	2500	1.03	97

[a] Determined by GPC. [b] Determined by ^{1}H NMR.[22]

distilled from calcium hydride under a N_2 atmosphere. 2,2′-Azobis(2-methylpropionitrile) (98%) (AIBN) was recrystallized from ethanol. Isobutylene (IB) (BOC, 99.5%) and CH_3Cl (Alexander Chemical Corp.) were dried through columns packed with $CaSO_4$ and $CaSO_4$/4 Å molecular sieves, respectively. Two monofunctional *exo*-olefin-terminated PIB precursors were synthesized using quasi-living polymerization of isobutylene followed by in situ quenching with 1,2,2,6,6-pentamethylpiperidine according to a previously reported method.[22] NMR spectra of these two polymers are shown in the Supporting Information, and their characterization results are summarized in Table 1.

The *exo*-olefin PIB precursors were converted into hydroxyl PIBs through hydroboration−oxidation as reported by Ivan et al.[23] The chain transfer agent, 4-cyano-4-(dodecylsulfanylthiocarbonylsulfanyl)pentanoic acid (CTA), was synthesized according to previously reported literature methods.[18]

Synthesis of 4-Cyano-4-(dodecylsulfanylthiocarbonylsulfanyl)pentanoic Acid-Functionalized PIB (PIB−CTA). To a 25 mL one-neck round-bottom flask equipped with a magnetic stir bar were added DCC (0.32 g, 1.54 mmol), DMAP (38 mg, 0.31 mmol), and CTA (0.39 g, 0.96 mmol) under a dry nitrogen atmosphere. In a separate vessel, hydroxyl-functional PIB-1 (1.25 g, 0.77 mmol) was dissolved in 13.5 mL of DCM, and the resulting solution was charged to the reaction flask. After 12 h, the reaction was filtered, and the solvent was removed under reduced pressure. The resulting product was dissolved in hexane, washed with methanol, and then precipitated into methanol from hexane. The precipitate was dissolved in hexane and washed first with a saturated NaCl solution and then with deionized water. The solution was then dried over magnesium sulfate and filtered, and the hexane was stripped under reduced pressure until a constant weight was reached.

Polymerization of MMA and S from PIB−CTA. A representative RAFT polymerization was conducted as follows. To a 25 mL Schlenk-style, long-neck round-bottom flask were charged

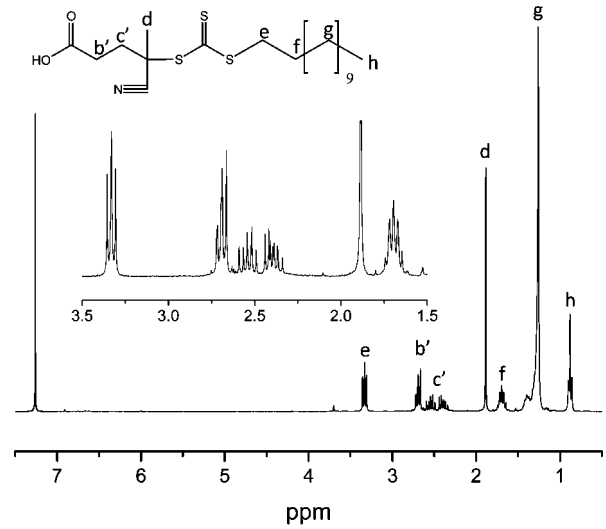

Figure 1. ^{1}H NMR spectrum of CTA.

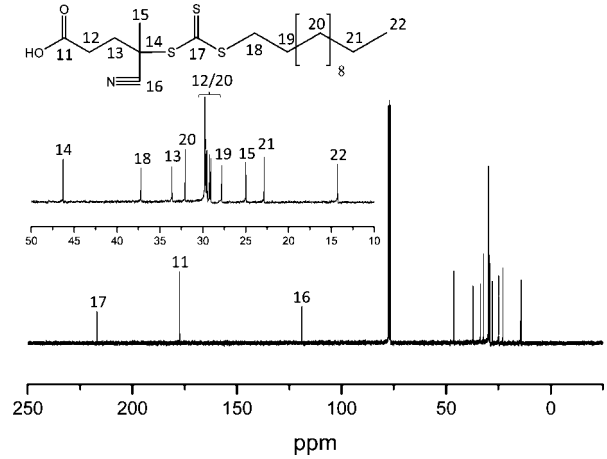

Figure 2. ^{13}C NMR spectrum of CTA.

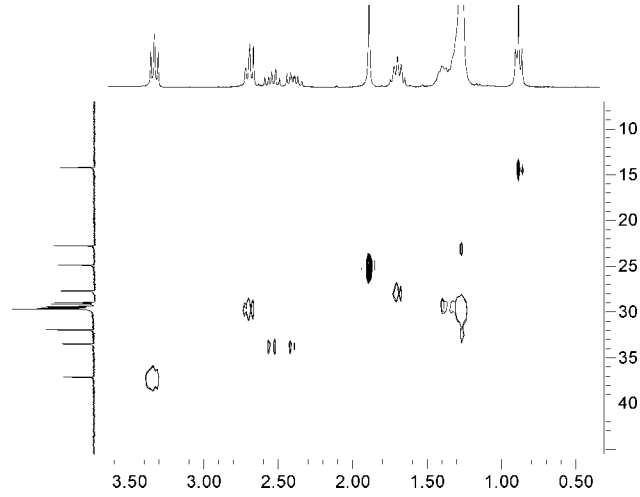

Figure 3. gHSQC of CTA.

PIB-1−CTA (0.069 g, 0.031 mmol), 1,3,5-trioxane (0.048 g, 0.533 mmol), MMA (0.394 g, 3.94 mmol), and AIBN (0.0025 g, 0.015 mmol) in 0.18 mL of benzene. After dissolution of the reagents an initial aliquot was taken to establish the initial monomer concentration relative to the internal standard 1,3,5-trioxane, via ^{1}H NMR spectroscopy. The solution was then subjected to three freeze−pump−thaw cycles to remove oxygen, sealed under N_2, and submerged in an oil bath at 60 °C. After

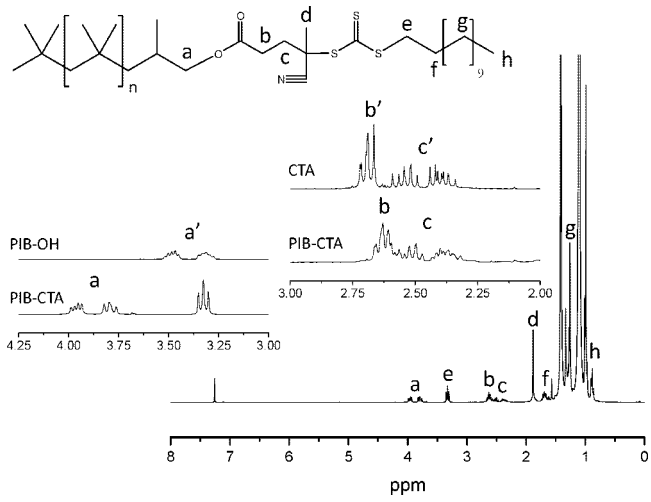

Figure 4. ^{1}H NMR spectrum of PIB−CTA.

~16 h the reaction was exposed to oxygen and quenched in liquid nitrogen. A final aliquot was taken for ^{1}H NMR analysis, and then the crude reaction product was precipitated into hexane and placed under vacuum until a constant mass was reached. Conversion was calculated from the initial and final monomer concentrations relative to 1,3,5-trioxane.

Instrumentation. NMR spectra were acquired using a Varian Mercury^{plus} 300 MHz NMR spectrometer. Samples were dissolved in chloroform-*d* (3−7%, w/v) and analyzed using 5 mm NMR tubes. ^{13}C and ^{1}H resonances were correlated with gradient enhanced heteronuclear single-quantum coherence (gHSQC) spectroscopy, using the average of 16 transients for each of 2 × 512 increments and phase-sensitive detection in the F1 dimension.

Variable-temperature NMR (VT NMR) data were acquired using a Varian Mercury^{plus} 300 MHz NMR spectrometer fitted with a Bruker Eurotherm VT controller. RAFT polymerizations were performed in benzene-*d* at 333 K, with a 250 s preacquisition delay between each spectrum. The probe was allowed to equilibrate for 10 min prior to data acquisition. Temperatures reported in this study are within ±2 deg based on ethylene glycol calibration.[24,25] RAFT polymerizations for VT NMR were prepared by first charging a Schlenk-style round-bottom flask with the crude reaction mixture and performing three freeze−thaw−pump cycles. After degassing, and just prior to analysis, the contents were transferred into an airtight NMR tube within a dry nitrogen atmosphere glovebox. Conversion was calculated by comparison of the vinyl proton areas of the monomer to the internal standard, 1,3,5-trioxane.

Number-average molecular weight (M_n) and polydispersity index (PDI) of the polymeric materials were measured using a gel permeation chromatography (GPC) system consisting of a Waters Alliance 2695 separation module, an online multiangle laser light scattering (MALLS) detector fitted with a gallium arsenide laser (power: 20 mW) operating at 690 nm (MiniDAWN, Wyatt Technology Inc.), an interferometric refractometer (Optilab DSP, Wyatt Technology Inc.), and two Polymer Laboratories mixed E columns (pore size range 50−10^3 Å, 3 μm bead size) connected in series. Freshly distilled THF served as the mobile phase and was delivered at a flow rate of 1.0 mL/min. Sample concentrations were ca. 6−7 mg of polymer/mL of THF, and the injection volume was 100 μL. The detector signals were simultaneously recorded using ASTRA software (Wyatt Technology Inc.), and absolute molecular weights were determined by MALLS. The d*n*/d*c* values for PIB homopolymer, PIB−CTA, PIB-*b*-poly(methyl methacrylate) (PIB-*b*-PMMA), and PIB-*b*-polystyrene (PIB-*b*-PS) were calculated from the response of the Optilab DSP and assuming 100% mass recovery from the columns.

Diblock Copolymer Molecular Weight and Blocking Efficiency by ^{1}H NMR. The number-average molecular weights of the diblock copolymers were calculated using ^{1}H NMR and eq 1 for PIB-*b*-PMMA and eq 2 for PIB-*b*-PS. $A_{methoxy}$ and $A_{aromatic}$ represent the area of the methoxy protons of PMMA and the aromatic protons of PS; M_{MMA} and M_S are the molecular weights of the corresponding monomer units, and $M_{n,PIB-CTA}$ equals 2200 g/mol for PIB-1 and 3100 g/mol for PIB-2. The methylene protons on carbon two of the CTA were used to normalize $A_{methoxy}$ and $A_{aromatic}$.

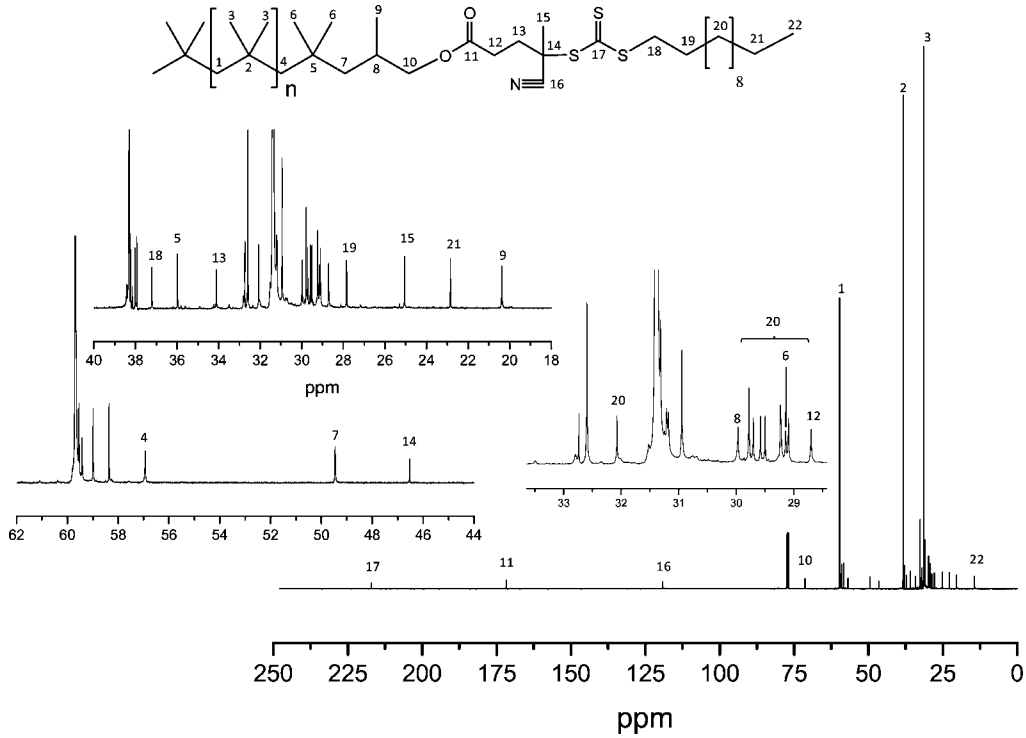

Figure 5. ^{13}C NMR spectrum of PIB−CTA.

$$M_{n,NMR} = \frac{A_{methoxy}}{3} \times M_{MMA} + M_{n,PIB-CTA} \quad (1)$$

$$M_{n,NMR} = \frac{A_{aromatic}}{5} \times M_S + M_{n,PIB-CTA} \quad (2)$$

Blocking efficiency (B_{eff} %) was calculated using GPC (eq 3) and ^{1}H NMR (eq 4).

$$B_{eff}\% = \frac{M_{n,theo} - M_{n,PIB-CTA}}{M_{n,GPC} - M_{n,PIB-CTA}} \quad (3)$$

$$B_{eff}\% = \frac{M_{n,theo} - M_{n,PIB-CTA}}{M_{n,NMR} - M_{n,PIB-CTA}} \quad (4)$$

$M_{n,GPC}$ is the number-average molecular weight of the diblock copolymer determined using GPC-MALLS. $M_{n,theo}$ is the theoretical number-average molecular weight of the diblock copolymer calculated according to eq 5 for PIB-*b*-PMMA (the calculation is analogous for PIB-*b*-PS), where p is monomer conversion for the RAFT polymerization and $[MMA]_0$ and $[PIB-CTA]_0$ refer to the initial MMA and PIB−CTA concentrations, respectively.

$$\frac{p[MMA]_0 M_{MMA}}{[PIB-CTA]_0} + M_{n,PIB-CTA} \quad (5)$$

Results and Discussion

The method employed for site transformation from living carbocationic polymerization to RAFT polymerization is shown in Scheme 1. The initial PIB block was synthesized by quasi-living cationic polymerization using the 2-chloro-2,4,4-trimethylpentane/$TiCl_4$ initiation system. After reaching full conversion of the IB monomer, in situ quenching with the hindered nucleophile, PMP, was used to convert the quasi-living cationic chain ends into *exo*-olefin functionality.[22] After quenching, ^{1}H NMR integration was used to characterize the end-group composition of the product by assuming that *tert*-chloride, *endo*-olefin, *exo*-olefin, and coupled PIB chain ends represent 100% of the chain ends. The results indicated that the PIB precursors were functionalized to near-quantitative amounts (Table 1) showing only trace quantities of *tert*-chloride, *endo*-olefin, and coupled products. Terminal *exo*-olefin PIB functionality was selected because of the convenience of in situ quenching and the facile transformation of this end group into a variety of other functional groups. Low molecular weight PIB was targeted in this work to facilitate accurate NMR analysis. For discussion purposes all NMR and GPC characterization results will correspond to PIB-1 (Table 1), unless otherwise stated. ^{1}H and ^{13}C NMR spectra of *exo*-olefin PIB are available in the Supporting Information, Figures 1 and 2, respectively. GPC traces of both the prequench *tert*-chloride PIB and quenched *exo*-olefin PIB are also available in Supporting Information, Figure 3.

Exo-olefin PIB was converted into hydroxyl PIB by hydroboration oxidation.[23] Complete characterization of hydroxyl PIB using ^{1}H/^{13}C NMR along with the GPC traces before and after functionalization demonstrated its successful synthesis (Supporting Information: Figures 4−6). From ^{1}H NMR the disappearance of the methylene (2.00 ppm), methyl (1.78 ppm), and olefinic protons (4.85 and 4.64 ppm) and formation of the new methylene protons (3.53−3.41 and 3.36−3.26 ppm) adjacent to the hydroxyl group indicated near-quantitative conversion from the *exo*-olefin PIB. ^{13}C NMR revealed that the *exo*-olefin carbons at 144.53 and 114.03 ppm were absent in the hydroxyl PIB, and new shifts for these carbons appeared at 31.99 and 69.86 ppm, respectively. Carbons immediately adjacent to the *exo*-olefin functionality also shifted from 53.87 to 49.58 ppm and from 25.91 to 20.04 ppm. The GPC traces, in Figure 6 of the Supporting Information, did not show significant changes in M_n and indicated the absence of any coupling.

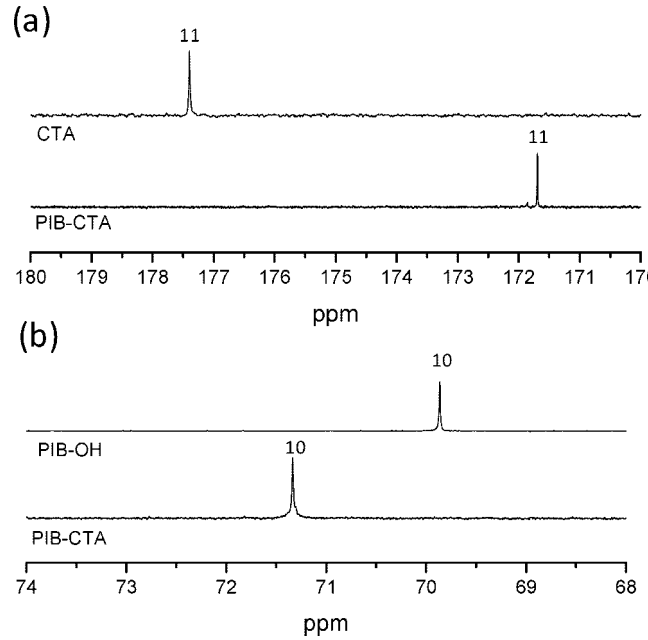

Figure 6. Partial ^{13}C NMR spectra comparing PIB−CTA to CTA and PIB−OH precursors.

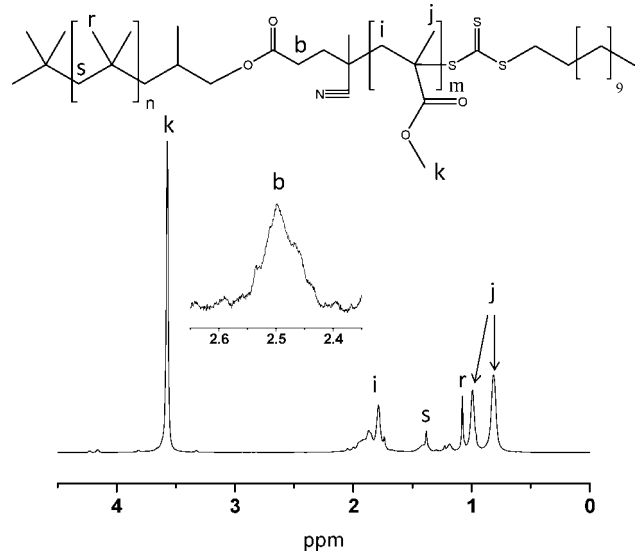

Figure 7. ^{1}H NMR spectrum of PIB-*b*-PMMA.

The CTA, 4-cyano-4-(dodecylsulfanylthiocarbonylsulfanyl)-pentanoic acid, was synthesized according to previously reported literature methods and characterized using ^{1}H and ^{13}C NMR, as shown in Figures 1 and 2. This particular CTA was chosen due to its solubility in low-polarity media, facile synthesis, reduced odor,[17] and established ability to polymerize MMA.[18] ^{1}H NMR peak assignments were obtained from the literature.[18]

^{13}C NMR peak assignments were made using two-dimensional gHSQC (Figure 3) and further bolstered by an attached proton test, which can be found in Figure 7 of the Supporting Information. In Figure 3, the carbon assignments were made by correlation with their respective proton peaks; although some ambiguity exists in identification of carbon 12 (associated with protons b′ in Figure 1) due to overlap of its signal with the numerous carbon peaks of the dodecyl group. Carbons 11, 14,

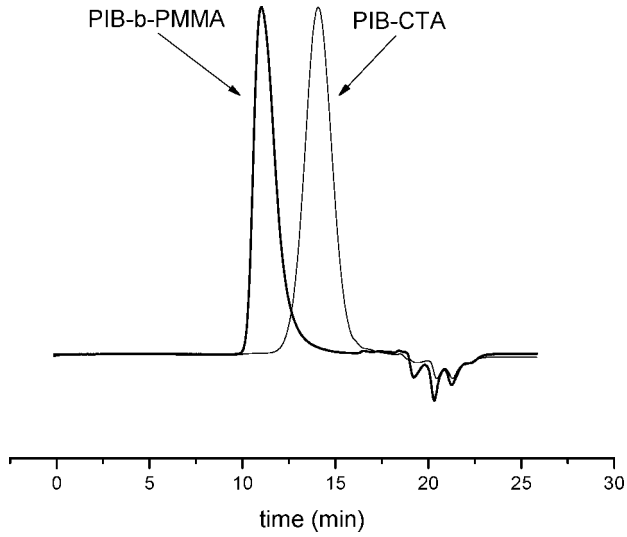

Figure 8. GPC traces of PIB−CTA and PIB-*b*-PMMA after purification.

16, and 17 had no correlations during the HSQC experiment, confirming that they were indeed quaternary carbons.

Synthesis of a PIB-based macro-CTA was accomplished by esterification of the CTA with hydroxyl PIB. The esterification reaction utilized DMAP as a catalyst and DCC as a water scavenger. This reaction successfully yielded CTA-functionalized PIB to near-quantitative conversion. Structural evidence of the resulting PIB−CTA can be seen in the ^{1}H and ^{13}C NMR spectra shown in Figures 4 and 5, respectively. In Figure 4, the methylene protons (a′) adjacent to the hydroxyl group on the PIB shifted from their original location at approximately 3.53−3.26 to 4.00−3.74 ppm. In addition, no residual methylene protons of the hydroxyl-terminated PIB were visible, indicating complete conversion was achieved. Also, the methylene protons (b′) adjacent to the acid functionality on the CTA shifted slightly upfield from their original location after coupling with the hydroxyl PIB.

In the ^{13}C NMR spectrum of the PIB−CTA (Figure 5) peaks from both the CTA and hydroxyl PIB are visible, indicating that both structures are present and coupled together after purification. If the CTA were not covalently attached to the PIB, it would have been removed during washing and precipitation of the polymer. Because of the number of peaks present in Figure 5, direct comparisons of expanded, partial spectra of the CTA, hydroxyl PIB, and PIB−CTA were performed for accurate identification of each peak. These expanded spectral comparisons can be found in Figures 8−10 of of the Supporting Information. Strong shifts were observed for the methylene carbon (C-10) adjacent to oxygen in the PIB precursor and the carbonyl carbon of the CTA (C-11), as displayed in Figure 6. After esterification, the methylene carbon shifted from 69.86 to 71.33 ppm; whereas the carbonyl carbon shifted from 177.39 to 171.69 ppm. No residual carbonyl carbon or methylene carbon peaks from the precursors were visible in the resulting product. Carbon atoms two and three bonds away also shifted slightly including C-9 (20.04 to 20.37 ppm) and C-8 (31.99 to 29.97 ppm) of hydroxyl PIB and C-12 (29.64 to 28.70 ppm) and C-13 (33.38 to 34.11 ppm) of the CTA.

Upon addition of the CTA to hydroxyl PIB a molecular weight increase should have been observed. GPC results confirmed that the PIB−CTA molecular weights were 2200 and 3100 g/mol for PIB-1 and PIB-2, respectively. These values are close to the predicted molecular weights after the coupling reaction.

Once the CTA-functionalized PIB was obtained, RAFT polymerizations were conducted for the synthesis of both PIB-*b*-PMMA and PIB-*b*-PS. Initial RAFT polymerizations were conducted with MMA using a variety of reaction conditions to optimize polymerization rate and blocking efficiency of the macro-CTA. This preliminary experimentation revealed that

Table 2. RAFT Polymerizations of PMMA and PS

	reaction conditions							M_n (g/mol)			blocking efficiency (%)	
exp	PIB−CTA	monomer	[M] (mol/L)	[M]:[CTA]:[I]	time[b] (h)	conv	PDI	GPC	NMR	theo	GPC	NMR
R-1	PIB-2	MMA	6.50	130:1:0.52	10.8	94.6	1.04	17 000	17 840	15 410	88.6	83.5
R-2	PIB-2	MMA	5.52	142:1:0.53	11.8	93.0	1.04	17 100	16 810	16 300	94.3	96.3
R-3	PIB-2	MMA	4.48	146:1:0.53	19	100	1.04	18 200	17 820	17 480	95.2	97.7
R-4	PIB-2	MMA	3.51	143:1:0.51	14.8	80.9	1.06	15 900	14 200	14 670	90.4	104.2
R-5	PIB-1	MMA	6.30	125:1:0.54	15.3	70.4	1.06	12 000	12 500	11 020	90.0	85.6
R-6	PIB-1	MMA	6.48	85:1:0.51	13.3	100	1.03	14 000	11 370	10 720	72.2	92.9
R-7	PIB-1	MMA	6.51	139:1:0.26	14	100	1.04	18 300	16 290	16 130	86.5	98.9
R-8[a]	PIB-2	S	bulk	301:1:0.0	20	82.2	1.02	26 700	26 160	28 910	109.4	111.9
R-9[a]	PIB-2	S	bulk	200:1:0.0	20.8	52.8	1.04	13 000	14 100	14 080	110.9	99.8

[a] Bulk polymerization of styrene with thermal initiation at 100 °C. [b] Elapsed time between initiation and quenching of RAFT polymerization.

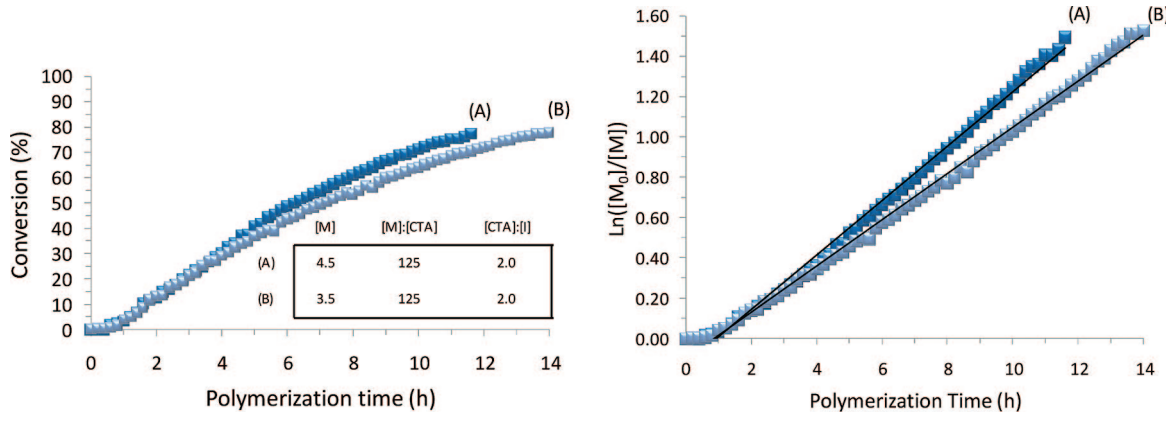

Figure 9. Effect of system concentration on rate of RAFT polymerization.

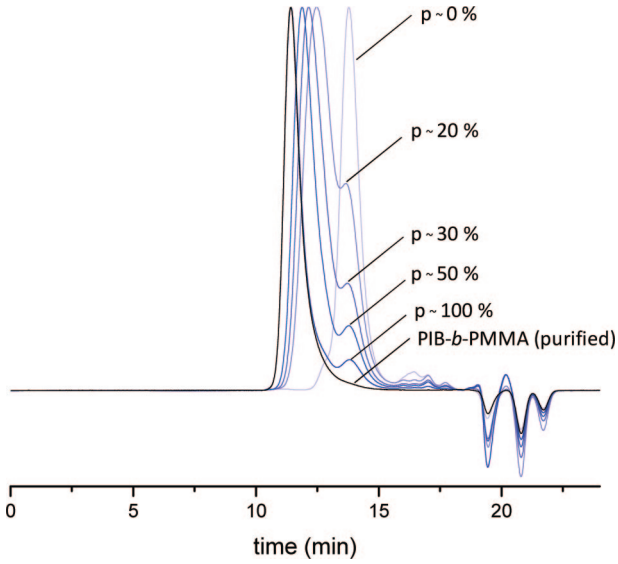

Figure 10. GPC traces of reaction aliquots removed from reaction R-3 at various conversions along with the final purified block copolymer.

monomer concentrations below 3 M and [CTA]:[AIBN] ratio above five resulted in unreasonably long reaction times and that lower temperatures (e.g., 60−70 °C) afforded increased blocking efficiency at the expense of longer reaction times. Figures 7 and 8 show the ^{1}H NMR spectrum and GPC traces, respectively, of a representative PIB-*b*-PMMA copolymer polymerized at optimal conditions, after purification. Because of the relatively long PMMA block, fractional precipitation of the crude reaction product into hexanes was effective at removing unreacted PIB−CTA. The ^{1}H NMR spectrum shows characteristic peaks from both PIB and PMMA. The CTA methylene proton peak (b) was used to normalize the methoxy peak of the PMMA for NMR molecular weight calculations. In addition, the GPC traces illustrate a substantial decrease in elution volume from the macro-PIB−CTA starting material to the PIB-*b*-PMMA, indicating an increase in molecular weight.

Next, a series of RAFT polymerizations was performed in which monomer concentration ([M]), [M]:[CTA]:[AIBN], and type of monomer were varied in order to probe their influence on blocking efficiency. Table 2 summarizes the conditions of each polymerization and its respective conversion, PDI, molecular weight, and blocking efficiency. Blocking efficiency was determined using both GPC and ^{1}H NMR as described in the Experimental Section.

Experiments R-1−R-4 were all conducted with near-identical [M]:[CTA]:[I] concentration ratios but differed in overall system concentration, which was dictated by the selected monomer concentration [M]. No clear trends can be observed concerning the blocking efficiency of the macro-CTA regarding the system concentration. It is possible that an optimal system concentration may exist at or around [M] = 4.5 M (R-3) indicated by blocking efficiencies greater than 95%. Additionally, less concentrated systems (R2−R4) resulted in slightly improved blocking efficiencies compared to that of the more concentrated system (R-1). The various polymerizations detailed in Table 2 demonstrate the capability of this system to yield targeted molecular weights over a fairly broad range (12000 to 18000 g/mol) and low PDIs, even when the polymerizations are taken to high monomer conversion.

Experiments R-3 and R-4 were divided into two portions prior to initiation. One portion was transferred into a round-bottom flask for a traditional RAFT polymerization and the other into an NMR tube for VT NMR. These VT NMR experiments were utilized to obtain real-time conversion and polymerization rate versus time data, as a function of system concentration, as shown in Figure 9. Except for an initial induction period, the RAFT polymerizations exhibited linear first-order plots, indicating an approximately constant number of growing species. Such an induction period is commonly observed in RAFT polymerizations[26,27] and is generally attributed to the establishment of the main RAFT equilibrium. As expected, the more concentrated system, curve A, achieved larger conversion values in the same duration of time, without causing any increase in PDI or decrease in the degree of molecular weight control (see data in Table 2). This shows that shorter reactions times can be achieved with higher system concentrations without deleterious effects to the resulting block copolymer.

In addition to monitoring the conversion of the system with ^{1}H NMR, aliquots were taken during the polymerization for GPC analysis. Figure 10 shows the GPC traces of reaction aliquots removed from reaction R-3 at various conversions, along with the final purified block copolymer. A gradual increase in molecular weight with conversion can be seen. At full conversion a small fraction of residual PIB−CTA remained in the crude reaction product. This residual fraction was isolated by fractional precipitation and found to contain some PMMA in its structure. This suggests that the failure of this fraction to form the desired second block may result from a combination

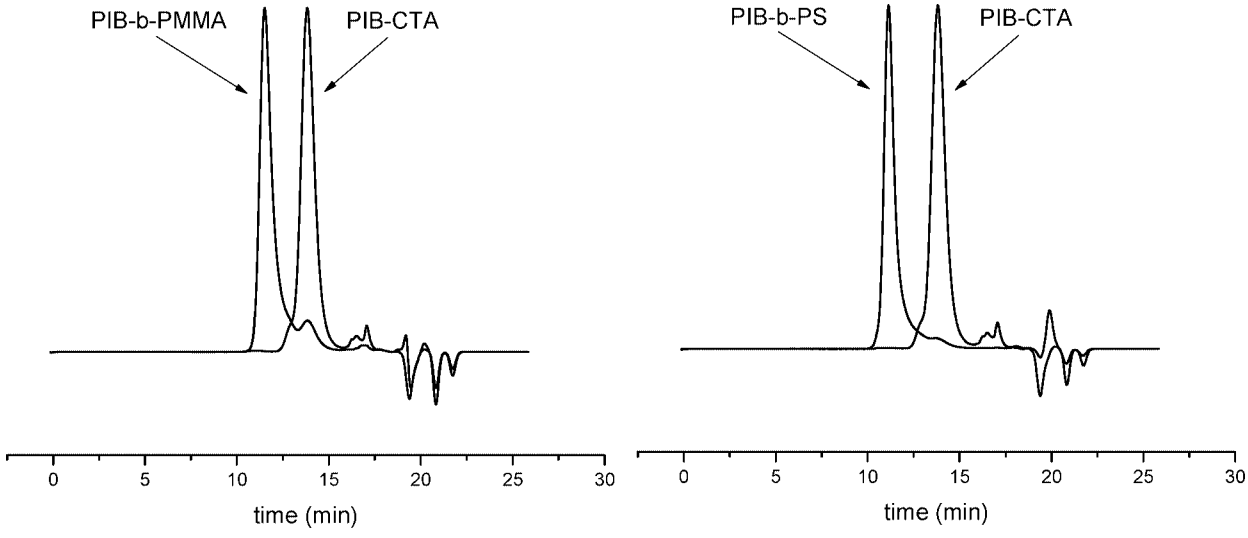

Figure 11. Dependency of blocking efficiency on monomer selection: MMA vs S.

of poor initiation efficiency, i.e., all MMA is consumed before all PIB−CTA's react, and early termination, resulting in a very short PMMA block.

To test whether the less-than-quantitative initiation efficiency might be due specifically to the selection of MMA, styrene was selected as a second monomer to conduct RAFT polymerization from the PIB macroinitiator. Styrene polymerization was conducted in the bulk, thereby simplifying the system greatly by elimination of solvent and initiator, and styrene polymerization has been shown to proceed in a controlled fashion in the RAFT process.[28] In Figure 11 the same PIB−CTA was used to polymerize MMA (R-1) and S (R-8). It is apparent that styrene yielded substantially improved blocking efficiency as evidenced by the significanly reduced amount of residual PIB−CTA. The molecular weight data in Table 2 show that styrene also yielded diblock copolymers with low PDI. However, the polymerization of styrene yielded experimental M_n values (both GPC and NMR) slightly lower than that of the theoretical value, giving apparent blocking efficiency values exceeding 100%.

Conclusion

Site transformation of PIB chain ends into functional macro-CTAs was successfully accomplished. The macro-CTA synthesized in this work represents the first report of combining cationic IB polymerization and subsequent RAFT polymerization for block copolymer synthesis. Structure of the macro-CTA was confirmed by both ^{1}H and ^{13}C NMR after coupling the CTA to PIB. RAFT polymerizations using the PIB−CTA were demonstrated with both MMA and S to yield block copolymers with predetermined molecular weights and narrow PDIs, as characterized by GPC and ^{1}H NMR. VT NMR experiments verified that MMA polymerizations progressed in a controlled fashion and that the rate was concentration dependent. Blocking efficiency values were found to be slightly improved with S compared MMA.

Supporting Information Available: NMR and GPC characterization of polyisobutylene precursors, CTA, and macro-CTA. This material is available free of charge via the Internet at http://pubs.acs.org.

References and Notes

(1) Kennedy, J. P. *J. Polym. Sci., Part A: Polym. Chem.* **2005**, *43*, 2951–2963.
(2) Ranade, S. V.; Miller, K. M.; Richard, R. E.; Chan, A. K.; Allen, M. J.; Helmus, M. N. *J. Biomed. Mater. Res.* **2004**, *71A*, 625–634.
(3) Pinchuk, L.; Wilson, G. J.; Barry, J. J.; Schoephoerster, R. T.; Parel, J.-M.; Kennedy, J. P. *Biomaterials* **2008**, *29* (4), 448–460.
(4) Cho, J. C.; Cheng, G.; Feng, D.; Faust, R.; Richard, R.; Schwarz, M.; Chan, K.; Boden, M. *Biomacromolecules* **2006**, *7* (11), 2997–3007.
(5) Sipos, L.; Som, A.; Faust, R.; Richard, R.; Schwarz, M.; Ranade, S.; Boden, M.; Chan, K. *Biomacromolecules* **2005**, *6* (5), 2570–2582.
(6) Binder, W. H.; Sachsenhofer, R. *Macromol. Rapid Commun.* **2008**, *29* (12−13), 1097–1103.
(7) Burkhardt, M.; Ruppel, M.; Tea, S.; Drechsler, M.; Schweins, R.; Pergushov, D. V.; Gradzielski, M.; Zezin, A. B.; Müller, A. H. E. *Langmuir* **2008**, *24* (5), 1769–1777.
(8) Binder, W. H.; Machl, D. *J. Polym. Sci., Part A: Polym. Chem.* **2005**, *43* (1), 188–202.
(9) Gao, L.-C.; Zhang, C.-L.; Liu, X.; Fan, X.-H.; Wu, Y.-X.; Chen, X.-F.; Shen, Z.; Zhou, Q.-F. *Soft Matter* **2008**, *4* (6), 1230–1236.
(10) Storey, R. F.; Scheuer, A. D.; Achord, B. C. *Polymer* **2005**, *46* (7), 2141–2152.
(11) Breland, L. K.; Storey, R. F. *Polymer* **2008**, *49* (5), 1154–1163.
(12) Kennedy, J. P.; Fang, Z. *J. Polym Sci., Part A: Polym. Chem.* **2002**, *40* (21), 3662–3678.
(13) Jakubowski, W.; Tsarevsky, N. V.; Higashihara, T.; Faust, R.; Matyjaszewski, K. *Macromolecules* **2008**, *41* (7), 2318–2323.
(14) Zaschke, B.; Kennedy, J. P. *Macromolecules* **1995**, *28* (13), 4426–4432.
(15) Martinez-Castro, N.; Lanzendörfer, M. G.; Müller, A. H. E.; Cho, J. C.; Acar, M. H.; Faust, R. *Macromolecules* **2003**, *36* (19), 6985–6994.
(16) Kwon, Y.; Faust, R.; Chen, C. X.; Thomas, E. L. *Macromolecules* **2002**, *35* (9), 3348–3357.
(17) Moad, G.; Rizzardo, E.; Thang, S. H. *Polymer* **2008**, *49* (5), 1079–1131.
(18) Moad, G.; Chong, Y. K.; Postma, A.; Rizzardo, E.; Thang, S. H. *Polymer* **2005**, *46* (19), 8458–8468.
(19) Shi, L.; Chapman, T. M.; Beckman, E. J. *Macromolecules* **2003**, *36* (7), 2563–2567.
(20) De Brouwer, H.; Schellekens, M. A. J.; Klumperman, B.; Monteiro, M. J.; German, A. L. *J. Polym. Sci., Part A: Polym. Chem.* **2000**, *38* (19), 3596–3603.
(21) Perrier, S.; Takolpuckdee, P.; Westwood, J.; Lewis, D. M. *Macromolecules* **2004**, *37* (8), 2709–2717.
(22) Simison, K. L.; Stokes, C. D.; Harrison, J. J.; Storey, R. F. *Macromolecules* **2006**, *39* (7), 2481–2487.
(23) Iván, B.; Kennedy, J.; Chang, V. S. C. *J. Polym. Sci., Polym. Chem.* **1980**, *18* (11), 3177–3191.
(24) English, A. D. *J. Magn. Reson.* **1984**, *57* (3), 491–493.
(25) Van Geet, A. L. *Anal. Chem.* **1968**, *40* (14), 2227–2229.
(26) De, P.; Gondi, S. R.; Sumerlin, B. S. *Biomacromolecules* **2008**, *9* (3), 1064–1070.
(27) Barner-Kowollik, C.; Buback, M.; Charleux, B.; Coote, M. L.; Drache, M.; Fukuda, T.; Goto, A.; Klumperman, B.; Lowe, A. B.; Mcleary, J. B.; Moad, G.; Monteiro, M. J.; Sanderson, R. D.; Tonge, M. P.; Vana, P. *J. Polym. Sci., Part A: Polym. Chem.* **2006**, *44* (2), 5809–5831.
(28) Mayadunne, R. T. A.; Rizzardo, E.; Chiefari, J.; Krstina, J.; Moad, G.; Postma, A.; Thang, S. H. *Macromolecules* **2000**, *33* (2), 243–245.

MA900070D